RESEARCH ARTICLE OPEN ACCESS

"Chocolate Chip Sign" on Susceptibility-Weighted Imaging

A Novel Neuroimaging Biomarker for HTRA1-Related Cerebral Small Vessel Disease

Shoichiro Ando,[1] Rie Saito,[2] Sho Kitahara,[1] Masahiro Uemura,[1] Yuya Hatano,[1] Masaki Watanabe,[3] Taisuke Kato,[4] Yosuke Ito,[3,5] Atchayaram Nalini,[6] Tomohiko Ishihara,[7] Shigeo Murayama,[8,9] Hironaka Igarashi,[3] Akiyoshi Kakita,[2] and Osamu Onodera[1,4]

Correspondence
Prof. Onodera
onodera@bri.niigata-u.ac.jp

Neurol Genet 2025;11:e200237. doi:10.1212/NXG.0000000000200237

Abstract

Background and Objectives

HTRA1-related cerebral small vessel disease (HRSVD) is a rare hereditary form of cerebral small vessel disease (CSVD) caused by *HTRA1* pathogenic variants. Diagnosing HRSVD without genetic testing is challenging because of the lack of distinctive imaging features and clinical symptoms, and even family history can be unclear in some cases with HRSVD. This study investigates whether susceptibility-weighted imaging (SWI) can identify useful diagnostic findings for HRSVD.

Methods

This retrospective study included 8 patients with HRSVD, 12 with cerebral autosomal dominant arteriopathy with subcortical infarcts and leukoencephalopathy (CADASIL), and 14 with sporadic CSVD (sCSVD). Two neurologists blinded to clinical data counted the number of hypointense dots around the midbrain on SWI. Receiver operating characteristic curve analysis evaluated the optimal threshold of the number that can distinguish HRSVD and CADASIL or sCSVD. In addition, histopathologic analysis including measurement of leptomeningeal vessel diameter and type III collagen deposition was performed on autopsied brains from 3 cases each of HRSVD, CADASIL, and sCSVD and control participants.

Results

Patients with HRSVD exhibited a significantly higher number of hypointense dots around the midbrain on SWI compared with CADASIL and sCSVD groups. A threshold of 5 or more dots, termed the "Chocolate Chip Sign," well distinguished HRSVD from CADASIL and sCSVD (area under the curve: 0.817, 95% confidence interval: 0.624–1.00). Three-dimensional SWI reconstruction and 7T MRI confirmed these dots as dilated extraparenchymal vessels. Histopathologic analysis revealed pronounced dilation of leptomeningeal veins with type III collagen accumulation specifically, in HRSVD brains.

Discussion

The Chocolate Chip Sign on SWI represents a novel and promising neuroimaging biomarker for HRSVD. This finding holds significant potential for facilitating early diagnosis, prompting timely genetic testing, and appropriate family screening for this rare genetic disorder.

MORE ONLINE

Videos

Supplementary Material

[1]Department of Neurology, Brain Research Institute, Niigata University, Japan; [2]Department of Pathology, Brain Research Institute, Niigata University, Japan; [3]Center for Integrated Human Brain Science, Brain Research Institute, Niigata University, Japan; [4]Department of Molecular Neuroscience, Brain Research Institute, Niigata University, Japan; [5]Department of Functional Neurosurgery, Nishiniigata Chuo Hospital, Niigata, Japan; [6]Department of Neurology, National Institute of Mental Health and Neurosciences, Bangalore, India; [7]Advanced Treatment of Neurological Diseases Branch, Endowed Research Branch, Brain Research Institute, Niigata University, Japan; [8]Brain Bank for Neurodevelopmental, Neurological and Psychiatric Disorders, United Graduate School of Child Development, Osaka University, Japan; and [9]Brain Bank for Aging Research (Neuropathology), Tokyo Metropolitan Institute of Geriatrics and Gerontology, Japan.

The Article Processing Charge was funded by the authors.

Glossary

ANOVA = analysis of variance; **AUC** = area under the curve; **CADASIL** = cerebral autosomal dominant arteriopathy with subcortical infarcts and leukoencephalopathy; **CARASIL** = cerebral autosomal recessive arteriopathy with subcortical infarcts and leukoencephalopathy; **CSVD** = cerebral small vessel disease; **FLAIR** = fluid-attenuated inversion recovery; **GRE** = gradient-echo sequence; **H&E** = hematoxylin and eosin; **HTRA1** = high-temperature requirement A1; **HRSVD** = HTRA1-related cerebral small vessel disease; **LMA** = leptomeningeal artery; **ROC** = receiver operating characteristic; **sCSVD** = sporadic cerebral small vessel disease; **SWI** = susceptibility-weighted imaging; **T2WI** = T2-weighted imaging.

Introduction

Cerebral small vessel disease (CSVD) encompasses a range of disorders affecting the small vessels of the brain, which can be either hereditary or sporadic.[1] The sporadic form is more common in the older population. One of the inherited forms of CSVD is cerebral autosomal recessive arteriopathy with subcortical infarcts and leukoencephalopathy (CARASIL). CARASIL is a rare, early-onset CSVD resulting from loss-of-function variants in both alleles of the *HTRA1* gene, which encodes a serine protease.[2] Furthermore, pathogenic variants in a single allele of *HTRA1* can contribute to late-onset CSVD.[3-7] Consequently, CSVD associated with CARASIL and heterozygous *HTRA1* pathogenic variants is collectively termed HTRA1-related cerebral small vessel disease (HRSVD).[5]

Imaging findings in HRSVD are generally nonspecific and resemble other forms of CSVD[5], whereas advanced CARASIL cases exhibit a distinctive "arc sign" on T2-weighted imaging.[8] Moreover, patients with HRSVD often lack characteristic clinical features such as alopecia and low back pain, commonly associated with CARASIL.[5,9] In addition, family history is frequently unclear, especially in CSVD cases with heterozygous *HTRA1* pathogenic variants. Therefore, it is challenging to identify CSVD patients with high prior probability of an HTRA1-positive result who should undergo genetic testing.

Susceptibility-weighted imaging (SWI) has proven to be valuable in detecting vessel changes in CSVD. For instance, the "vessel-cluster sign,"[10] dilated small deep parenchymal vessels, has been reported in cerebral autosomal dominant arteriopathy with subcortical infarcts and leukoencephalopathy (CADASIL), and reduced visibility of deep medullary veins has been observed in CSVD.[11] However, SWI findings in HRSVD have not been comprehensively evaluated.

This study aims to investigate the potential diagnostic utility of a novel imaging marker, the "Chocolate Chip Sign," characterized by multiple hypointense dots around the midbrain on SWI, observed in patients with HRSVD. We also extended 7T high-resolution SWI and histopathologic study to explore the underlying pathophysiology of "Chocolate Chip Sign."

Methods

Patients for MRI Analysis

This study retrospectively analyzed 350 patients with CSVD who were referred for genetic analysis at the Brain Research Institute, Niigata University, from October 2010 to March 2022 (Figure 1). First, patients were classified into 3 groups: *NOTCH3*-positive group, *HTRA1*-positive group, and *NOTCH3* and *HTRA1* NOT-confirmed group. In the *NOTCH3*-positive group, the cysteine-sparing variants were excluded except for p.R75P.[12] In the *HTRA1*-positive group, the variants without previous confirmation of reduced protease activity[4,6,13] were excluded except for *HTRA1* p.V221A specifically confirmed in this study (eFigure 1, A and B). In the *NOTCH3* and *HTRA1* NOT-confirmed group, only patients who underwent whole-exome sequencing (WES) and showed no pathogenic variants related to CSVD were included. Exclusion criteria throughout the groups were as follows: no SWI or fluid-attenuated inversion recovery/T2-weighted imaging (FLAIR/T2WI) data, large cerebral hemorrhagic lesions (>15 mm), Fazekas grade ≤2 for both periventricular and deep white matter hyperintensities,[14] and arterial stenosis of the main trunk (if MR angiography data were available). The final patient cohort is presented in eTable 1.

Analysis of Hypointense Dots Around the Midbrain on SWI

Two board-certified neurologists (S.A. and S.K.) blinded to the patients' clinical details conducted the analysis. The number of hypointense dots was counted at a single midbrain level in 2 steps: 2 raters independently counted the number of dots, and then, the statistical analysis was performed using their lower values to avoid overestimating the number of dots. A comparison of the FLAIR/T2WI images confirmed that the hypointense dots were outside the parenchyma. The number of hypointense dots around the midbrain for each case is provided in eTable 2. Inter-rater reliability was evaluated using the weighted kappa coefficient.

Three-Dimensional Reconstruction of SWI Data

Three-dimensional (3D) reconstruction of the low signal on the brain surface was performed using SWI in the cases of HRSVD and CADASIL. The brains were extracted from the SWI scans using HD-BET. The extracted brain images were analyzed using a 3D Frangi vesselness filter in MATLAB

Figure 1 Flowchart of Selection of Patients

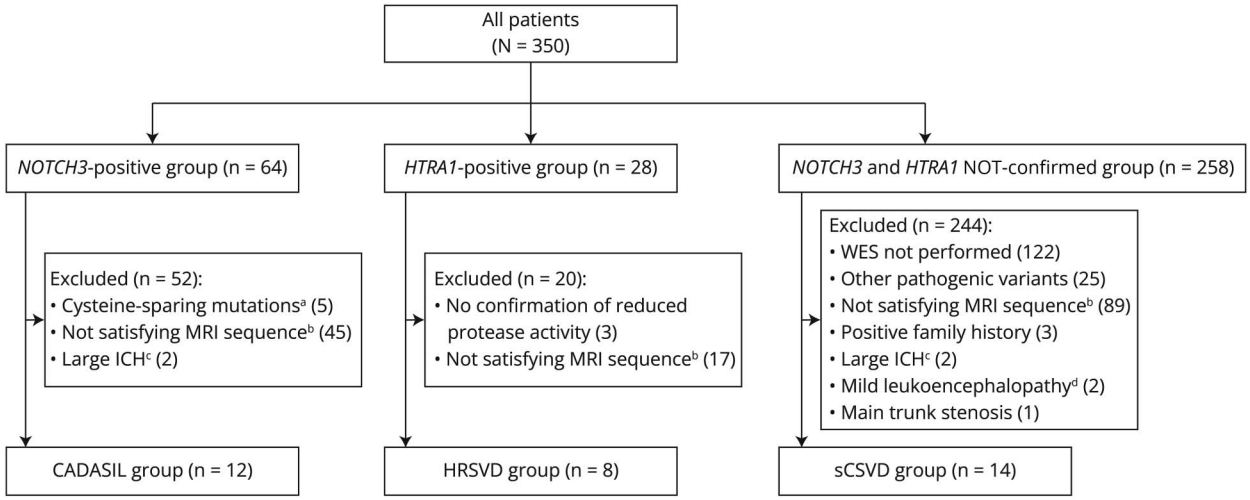

(A) Except for NOTCH3 p.R75P. (B) Susceptibility-weighted imaging (SWI) and fluid-attenuated inversion recovery (FLAIR) or T2-weighted imaging (T2WI) are required. (C) More than diameter of 15 mm. (D) Fazekas grade ≤2 in both deep white matter hyperintensities and periventricular hyperintensities. CADASIL = cerebral autosomal dominant arteriopathy with subcortical infarcts and leukoencephalopathy; HRSVD = HTRA1-related cerebral small vessel disease; ICH = intracranial hemorrhage; sCSVD = sporadic cerebral small vessel disease; WES = whole-exome sequencing.

(MathWorks, Natick, MA).[15-17] The parameters were set to default values. To generate high-quality images in TIFF format, we multiplied the voxel values of the analyzed data with the Frangi filter by a factor of 1000. The integer values were determined using the cast function in MATLAB, and any structures deemed to be venous sinuses or veins were removed manually. The resulting data were converted into TIFF images and loaded into Imaris 9.9.0 (Oxford Instruments, Abingdon, United Kingdom).

7-T High-Resolution MRI Study

High-spatial-resolution SWI using 7T MRI was conducted for HRSVD (Case 6 in eTable 1). The mesoscopic SWI study used a 7T Signa Horizon LX MRI system equipped with a 32-channel multielement coil for radiofrequency transception.[18,19] High-resolution T2*-weighted two-dimensional (2D) gradient-echo sequence (GRE) images were obtained using the following parameters: repetition time = 280 ms, echo time = 31.5 ms, flip angle = 40°, field of view = 80 × 80 mm, and matrix size = 512 × 512 with 3-mm thickness and 1-mm gap (0.156 × 0.156 × 3 mm in spatial resolution). The SWI scans were obtained by postprocessing the T2*-weighted 2D GRE images[20,21] using in-house software written in MATLAB 2019b on a window-based computer.

Pathologic Study

Immunohistochemical analysis was conducted for each of the 3 autopsied patients with HRSVD, CADASIL, and sporadic CSVD (sCSVD) and non-CSVD control participants without neurologic disorders. The profiles of these patients are summarized in eTable 3. Brains were fixed with 10% buffered formalin, and multiple tissue blocks were embedded in paraffin. Histologic examination was performed on 4-μm thick sections using hematoxylin and eosin (H&E) and Klüver-Barrera staining. Selected sections were immunostained with antibodies against type III collagen (Abcam, Cambridge, United Kingdom; 1:1000) and ferritin light chain (Abcam; 1:100). Antibodies against amyloid β 11–28 (IBL, Gunma, Japan; 1:50), phosphorylated tau (Fujirebio, Gent, Belgium; 1:200), and phosphorylated α-synuclein (Wako, Saitama, Japan; 1:1000) were used to assess senile pathologic changes and cerebral amyloid angiopathy (CAA) based on the 'ABC' score,[22] the fourth consensus report of the Dementia with Lewy Bodies Consortium,[23] and the CAA score.[24] Bound antibodies were visualized by a peroxidase polymer–based method using a Histofine Simple Stain MAX-PO kit (Nichirei, Tokyo, Japan), with diaminobenzidine as the chromogen. Immunostained sections were counterstained with hematoxylin.

We quantified venous diameter in the subarachnoid space of the midbrain. The veins were observed using Elastica-Goldner–stained sections under a ×10 objective lens, and images of all areas were digitized using an automated imaging system (NanoZoomer S60, Hamamatsu, Japan). In 5 of the 12 cases, sections were prepared from the half-cut midbrain, and the total number of leptomeningeal veins taken from the sections in each case was 583. Subsequently, the outer diameter of the veins in the subarachnoid space (leptomeningeal veins) was measured at 2 different points as previously described,[25] and the diameter was calculated as the average of the 2 measurements.

HTRA1 Digestion Assay

Full-length human type III collagen A1 (Novus Biologicals, H00001281-P01) and C-terminal myc-His6-tagged full-

length human HTRA1 protein (expressed in FreeStyle 293 cells and purified as previously described) were used in this study.[4] In brief, collagen A1 (100 ng) and varying concentrations of HTRA1 were incubated in the digestion buffer at 37°C for 6 hours. Cleavage activity was assessed by immunoblotting as previously described.[26]

Statistical Analysis

Statistical analysis was performed using Shapiro-Wilk, Welch, Kruskal-Wallis, Fisher exact, and Mann-Whitney *U* tests, as appropriate for data type and distribution. The Spearman rank correlation coefficient between disease duration and the number of hypointense dots in the HRSVD group was calculated. Receiver operating characteristic (ROC) curve analysis was used to assess the discriminative power of hypointense dots on SWI for predicting Chocolate Chip Sign positivity, and binomial logistic regression was used to adjust for disease duration and hypertension. Missing data were excluded for these statistical analyses. Statistical significance was set at $p < 0.05$. All analyses were conducted using EZR version 4.2.2 (Jichi Medical University, Saitama, Japan), XLSTAT (Denver, CO), and GraphPad Prism software version 9.5.1 (Boston, MA).

Ethics Approval

This study was approved by the Ethics Board of Niigata University (approval ID numbers 801, 802, and G2020-0032). Informed consent was obtained from all the participants.

Guidelines

We prepared our article in accordance with the Strengthening the Reporting of Observational Studies in Epidemiology (STROBE) cross-sectional study guidelines. A checklist is provided in eAppendix 1.

Data Availability

The corresponding author provides data related to this study on reasonable request.

Results

Clinical and Genetic Characteristics

Thirty-four patients were included in this study (HRSVD, n = 8; CADASIL, n = 12; and sCSVD, n = 14). The average age at onset was 37.6 years for HRSVD (range: 22–53 years), 45.7 years for CADASIL (range: 32–66 years), and 48.9 years for sCSVD (range: 30–64 years). The number of women was 2 (25.0%) in HRSVD, 5 (42.0%) in CADASIL, and 3 (21.0%) in sCSVD. The study participants were predominantly Japanese, except for one patient from Korea in the CADASIL group and 3 patients from India in the HRSVD group. Detailed clinical and genetic characteristics are presented in Table 1 and eTable 1. Data on hypertension, diabetes mellitus, dyslipidemia, smoking, and alcohol use were missing for one patient with sCSVD (Case No. 34). No significant differences were observed in the age at onset or the time from onset to MRI between the groups. Hypertension was more common in patients with sCSVD ($p = 0.008$), and dementia was more frequent in patients with CADASIL ($p = 0.026$).

Hypointense Dots Around the Midbrain in HRSVD

On SWI, numerous small, round-to-oval hypointense dots were predominantly observed surrounding the midbrain in patients with HRSVD (Figure 2, A and B, eFigure 2, A and B). This pattern, resembling scattered chocolate chips, was quantified at a single midbrain level by 2 independent raters (weighted $\kappa = 0.970$). Patients with HRSVD exhibited a significantly higher number of hypointense dots compared with patients with CADASIL or sCSVD ($p < 0.001$; Figure 2C). However, no significant correlation was found between disease duration and the number of hypointense dots in the HRSVD group (rs = 0.187, 95% confidence interval: −0.601-0.791, $p = 0.703$). A threshold of 5 or more dots, termed the Chocolate Chip Sign, demonstrated optimal sensitivity and specificity for differentiating HRSVD (area under the curve [AUC]: 0.817; 95% confidence interval [CI]: 0.624–1.00; Figure 2D, eTable 4), which remained significant even after adjusting for disease duration and hypertension (Table 2).

Continuous Characteristics of Hypointense Dots on SWI

3D reconstruction of hypointense signals in HRSVD and CADASIL revealed continuous, partially dilated structures, suggesting a vascular origin (Figure 3, A and B, Videos 1 and 2). High-resolution 7T SWI in a patient with HRSVD further demonstrated the extraparenchymal location of these hypointense dots (Figure 3C), supporting that hypointense dots seen on SWI represent superficial vessels.

Venous Dilation in Autopsied Brain With HRSVD

Histologic examinations were performed for the HRSVD, CADASIL, sCSVD, and control groups. In HRSVD, leptomeningeal veins exhibited partial dilation and wall thickening compared with the arteries (Figure 4A). Conversely, veins in CADASIL and sCSVD groups were uniformly and only slightly dilated with wall thickening relative to the arteries (eFigure 3, A–C). Dilated and thickened venous walls were also observed in the leptomeningeal region at the temporal tip (Figure 4B). Leptomeningeal venous diameter around the midbrain was significantly dilated in the HRSVD group compared with sCSVD and control groups (Figure 4D). It is important to note that the arterial diameter did not differ between HRSVD and the other 3 groups (CADASIL, sCSVD, and control) (Figure 4E). Ferritin staining of leptomeningeal vessels was performed to investigate whether the hypointense signal on SWI resulted from paramagnetic elements. Ferritin deposition in the leptomeningeal vessels in HRSVD was unremarkable compared with that in CADASIL and sCSVD (eTable 5).

Table 1 Clinical Characteristics of the Participants in the MRI Study

	HRSVD	CADASIL	Sporadic CSVD	*p* Value
Total number	8	12	14	
Age at onset (y/o)	37.6 (±11.4)	45.7 (±8.50)	48.9 (±10.3)	0.134[a]
Disease duration (y)	7.75 (±8.00)	3.10 (±3.00)	2.20 (±3.70)	0.092[b]
Sex (female)	2 (25.0%)	5 (42.0%)	3 (21.0%)	0.629[c]
Hypertension	1 (12.5%)	2 (16.7%)	9 (64.3%)	0.008[c]
Diabetes mellitus	0 (0%)	1 (8.30%)	1 (7.10%)	1.000[c]
Dyslipidaemia	0 (0%)	3 (25.0%)	4 (28.6%)	0.237[c]
Alcohol	0 (0%)	0 (0%)	2 (14.2%)	0.326[c]
Smoking	3 (37.5%)	7 (58.3%)	7 (50.0%)	0.747[c]
Gait disturbance	7 (87.5%)	5 (42.0%)	10 (71.4%)	0.113[c]
Dementia	1 (12.5%)	7 (58.3%)	2 (14.2%)	0.026[c]
Symptomatic CI	3 (37.5%)	8 (66.7%)	8 (57.1%)	0.467[c]
Symptomatic ICH	1 (12.5%)	1 (8.30%)	1 (7.10%)	1.000[c]
Fazekas grade (PVHs)	2: 0 (0%) 3: 8 (100%)	2: 2 (16.7%) 3: 10 (83.3%)	2: 1 (7.10%) 3: 13 (92.9%)	1.000[c]
Fazekas grade (DWMHs)	2: 0 (0%) 3: 8 (100%)	2: 2 (16.7%) 3: 10 (83.3%)	2: 1 (7.10%) 3: 13 (92.9%)	1.000[c]

Abbreviations: CSVD = cerebral small vessel disease; CI = cerebral infarction; DWMHs = deep white matter hyperintensities; HRSVD = HTRA1-related cerebral small vessel disease; ICH = intracranial hemorrhage; PVHs = perivascular hyperintensities; y/o = years old.
Data are presented as the mean ± SD or number of cases and percentages.
[a] Welch test for normally distributed variables.
[b] Kruskal-Wallis test for non-normally distributed variables.
[c] Fisher exact test for categorical variables.

Type III Collagen Accumulation in HRSVD

Because venous abnormalities in CSVD are characterized by aberrant type III collagen accumulation, immunostaining for type III collagen was performed.[27-29] Strong positivity for type III collagen was observed in thickened vascular walls on the brain surface, medullary veins, and capillaries in HRSVD, CADASIL, and sCSVD, but not in nondisease control (Figure 4C).

Because HTRA1 partially digests type III collagen,[29] we investigated whether HTRA1 digests full-length type III collagen and found that HTRA1 efficiently digested type III collagen in a concentration-dependent manner (eFigure 4).

Discussion

This study identifies a novel imaging marker for HRSVD termed the Chocolate Chip Sign. This sign, characterized by multiple hypointense dots surrounding the midbrain on SWI, exhibits potential for both the diagnosis and understanding of the pathophysiology of HRSVD. Our findings demonstrate that the Chocolate Chip Sign effectively differentiates HRSVD from CADASIL and sCSVD, thereby highlighting its utility as a diagnostic tool.

The evidence shown in this study suggests that these hypointense dots on SWI represent dilated veins rather than microbleeds. First, 3D reconstructions revealed a linear and tubular morphology that traces anatomical venous courses, in contrast to the typical punctate appearance of microbleeds. Second, high-field 7T MRI confirmed their extraparenchymal location, consistent with venous anatomy and aligning with histologic observations of venous dilation. Third, the pronounced hypointensity on SWI aligns with the known paramagnetic properties of deoxyhemoglobin, which are amplified in dilated veins.[20,30] This observation is further supported by the abundant superficial venous network around the midbrain,[30] making it an atypical location for marked presence of microbleeds.

While the Chocolate Chip Sign shows promise as a diagnostic marker for HRSVD, it is crucial to consider other conditions that may present with similar SWI features. CAA can exhibit multiple hypointense dots on SWI, typically representing microbleeds. However, they are usually distributed more diffusely throughout the cerebral cortex and subcortical white matter. The presence of lobar intracerebral hemorrhage or cortical superficial siderosis can also be a clue for distinguishing CAA from HRSVD.[31] In addition, other rare genetic small vessel diseases, such as COL4A1-related CSVD,

Figure 2 Hypointense Dots on Susceptibility-Weighted Imaging in Patients With HTRA1-Related Cerebral Small Vessel Disease

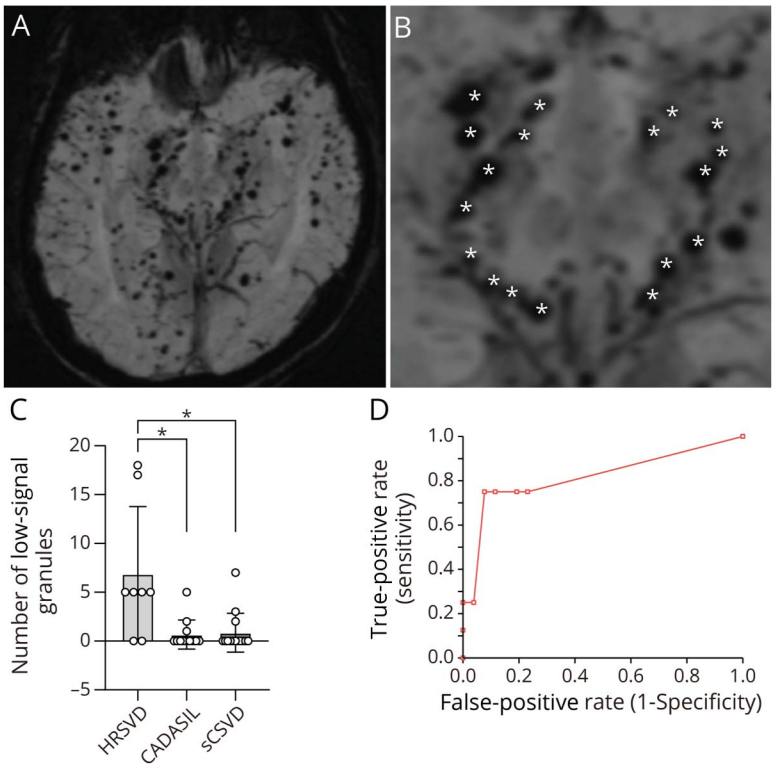

(A) Multiple hypointense dots are observed throughout the brain on susceptibility-weighted imaging (SWI); however, this finding is more prominent around the midbrain in a patient with homozygous HTRA1 p.E247Rfs. (B) The number of hypointense dots around the midbrain is counted at a single midbrain level by 2 board certified neurologists. The white asterisks indicate the actual counted dots. (C) The number of hypointense dots significantly increases in the HRSVD group (asterisks represent $p < 0.05$). (D) Receiver operating characteristic (ROC) curve of the number of hypointense dots is shown. The most suitable number of hypointense dots distinguishing HRSVD and non-HRSVD is found to be 5, with an area under the curve (AUC) of 0.817 (95% CI, 0.624–1.00), which is named as Chocolate Chip Sign. CADASIL = cerebral autosomal dominant arteriopathy with subcortical infarcts and leukoencephalopathy; HRSVD = HTRA1-related cerebral small vessel disease; sCSVD = sporadic cerebral small vessel disease.

may occasionally present with multiple hypointense dots on SWI.[32] To avoid misdiagnosis, it is essential to evaluate the Chocolate Chip Sign alongside other clinical and imaging features, family history, and, when appropriate, genetic testing. The presence of alopecia, spondylosis, or a family history of early-onset stroke would further support the diagnosis of HRSVD over other CSVDs.

We observed variability in the Chocolate Chip Sign, specifically in the number of hypointense dots around the midbrain among HRSVD cases. A previous study showed clinical heterogeneity of HRSVD, particularly among patients with heterozygous HTRA1 pathogenic variants. This may partially account for the discrepancies in the number of hypointense dots between individual HRSVD cases.[5] Although a correlation between disease duration and the number of hypointense dots was suggested, no statistically significant relationship was identified. Furthermore, it is noteworthy that one rater counted zero to 2 dots in patients with CARASIL. One possible explanation for these results may lie in factors not assessed in this study, including rare variants associated with monogenic hereditary CSVD, which are known to modify CSVD phenotypes.[33] Future studies exploring the association between other rare variants and the Chocolate Chip Sign in patients with HRSVD may provide valuable insights to address these unresolved questions.

Table 2 Binomial Logistic Regression Analysis Between HTRA1-Related Cerebral Small Vessel Disease (HRSVD) Group and Non-HRSVD Group

	Odds ratio	95% CI	*p* Value
CCS positivity	0.0294	0.00171–0.500	0.0149
Disease duration	0.957	0.731–1.25	0.752
Hypertension	8.69	0.430–175	0.159

Beyond its diagnostic value, the Chocolate Chip Sign provides critical insight into the pathophysiology of HRSVD. Our study observed extensive type III collagen deposition within the venous walls of patients with HRSVD. This aligns with previous studies linking similar collagen accumulation to venous collagenosis in sCSVD[27,28] and is further strengthened by the connection between matrisome protein accumulation, a hallmark of HRSVD.[26] Previous studies have shown that the accumulation of matrisome proteins leads to reduced elasticity and dilation of leptomeningeal arteries.[26] A similar mechanism may occur in the venous system, where type III collagen accumulation could compromise the structural integrity of venous walls, resulting in venous dilation. While our study focused on the accumulation of type III collagen in the

Figure 3 Hypointense Dots on Susceptibility-Weighted Imaging Indicate the Abnormal Cerebral Surface Veins

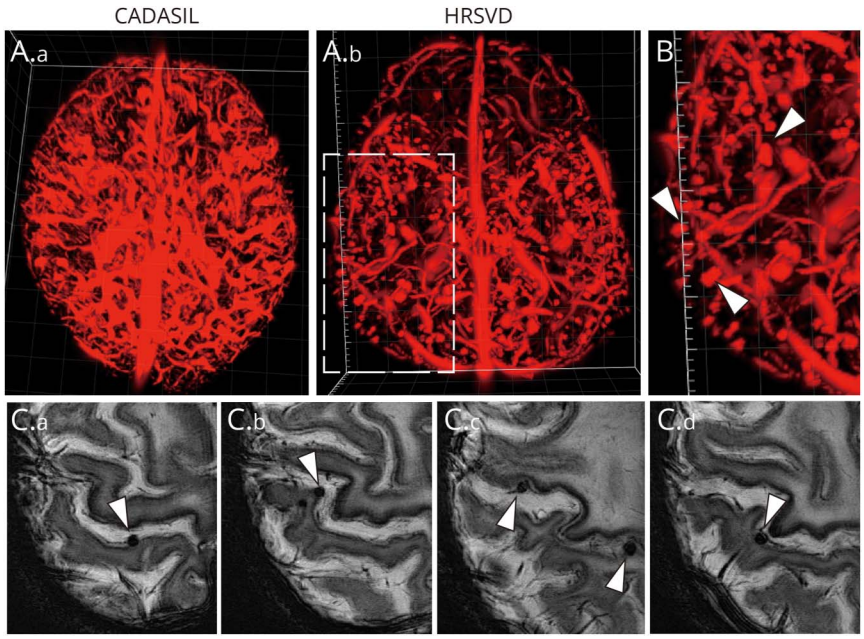

(A) Three-dimensional (3D) reconstruction of the hypointense dots on susceptibility-weighted imaging (SWI) is shown. Index cases include cerebral autosomal dominant arteriopathy with subcortical infarcts and leukoencephalopathy (CADASIL, a patient in their 40s with heterozygous NOTCH3 p.R169C, A.a) and HTRA1-related cerebral small vessel disease (HRSVD, a patient in their 20s with homozygous HTRA1 p.E247Rfs, A.b). A continuous linear structure is observed throughout the brain in CADASIL. (A.a). By contrast, these are interrupted and recognized as partial dilations in cases of HRSVD. (A.b). The reconstructed 3D images from all angles are shown in Videos 1 and 2, respectively. (B) Magnified image of the white dashed line in A.b. The hypointense area on SWI shows partial continuity, suggesting that it might be of vessel origin. These continuous structures demonstrate partially dilated and stenotic changes (B, arrowheads). (C) Hypointense dots are clearly detected on high-resolution 7T MRI outside the brain parenchyma in a patient with HRSVD (a patient with heterozygous HTRA1 p.R302Q) (arrowheads).

cerebral veins of patients with HRSVD, it is possible that other matrisome proteins, including fibronectin, may also play a role in the pathogenesis of this disease. Previous studies have shown that fibronectin accumulation is a key feature in HTRA1-deficient mouse models of HRSVD.[26] Indeed, immunostaining for fibronectin was also positive in venous walls in HRSVD, CADASIL, and sCSVD (data not shown). We propose that the loss of HTRA1 function, a key characteristic of HRSVD, disrupts the degradation of its substrates, including type III collagen, leading to excessive collagen accumulation and subsequent dilation of vascular walls. Although the accumulation of type III collagen and fibronectin within the venous walls was not limited to HRSVD in this study, further investigation with a larger sample size is warranted and the evaluation of other matrisome proteins would be valuable. Finally, the potential of candesartan to normalize fibronectin accumulation and vessel diameter in HTRA1-deleted mouse models offers a promising therapeutic strategy for HRSVD.[26] In this context, the Chocolate Chip Sign, a potential imaging biomarker reflecting this underlying pathophysiology, could serve as a valuable tool for monitoring treatment response in future clinical trials of candesartan for HRSVD.

Although the importance of type III collagen accumulation and venous dilation has been suggested, we were unable to examine the direct relationship between the extent of these pathologic findings and disease severity or progression because of the small sample size. A previous autopsy study demonstrated a significant association between periventricular venous collagenosis and a high prevalence of severe white matter lesions.[27] In addition, an MRI-based study indicated that the dilation of Rosenthal veins correlated with an increase in white matter lesion volume.[34] These observations suggest that the accumulation of type III collagen and venous dilation in HRSVD may not be coincidental but could represent a pathogenic mechanism that exacerbates the clinical severity. While the underlying mechanisms remain unclear, one plausible explanation is that these venous abnormalities might lead to dysfunction of the glymphatic system, which, in turn, exacerbates CSVD phenotypes.[35] Future investigations are needed to comprehensively examine the relationship between type III collagen accumulation and clinical severity or progression in HRSVD.

This study had several limitations. First, the small sample size of patients with HRSVD (n = 8) and the retrospective design limit the generalizability of our findings and the statistical power of our analyses. In addition, the study population was limited to only 2 ethnic groups. Therefore, a larger, multicenter, prospective study involving a more diverse population is required to validate the Chocolate Chip Sign as a reliable biomarker for HRSVD. Second, a significant limitation of our study is the inconsistency in SWI protocols across institutions. Generally, SWI protocols and parameters for 3T MRI include echo time of 20 ms, repetition time of 30 ms, flip angle of 15°, bandwidth of 120 Hz/pixel, and voxel size of 0.67 × 0.67 × 1.3 mm.[3,36] However, it is important to recognize that optimal SWI protocols can vary between MRI devices and institutions, leading to discrepancies in the lesion visualization and variability in identifying the Chocolate Chip Sign. To address this issue, future research should aim to standardize MRI device and

Figure 4 Leptomeningeal Venous Pathology in Patients With HTRA1-Related Cerebral Small Vessel Disease

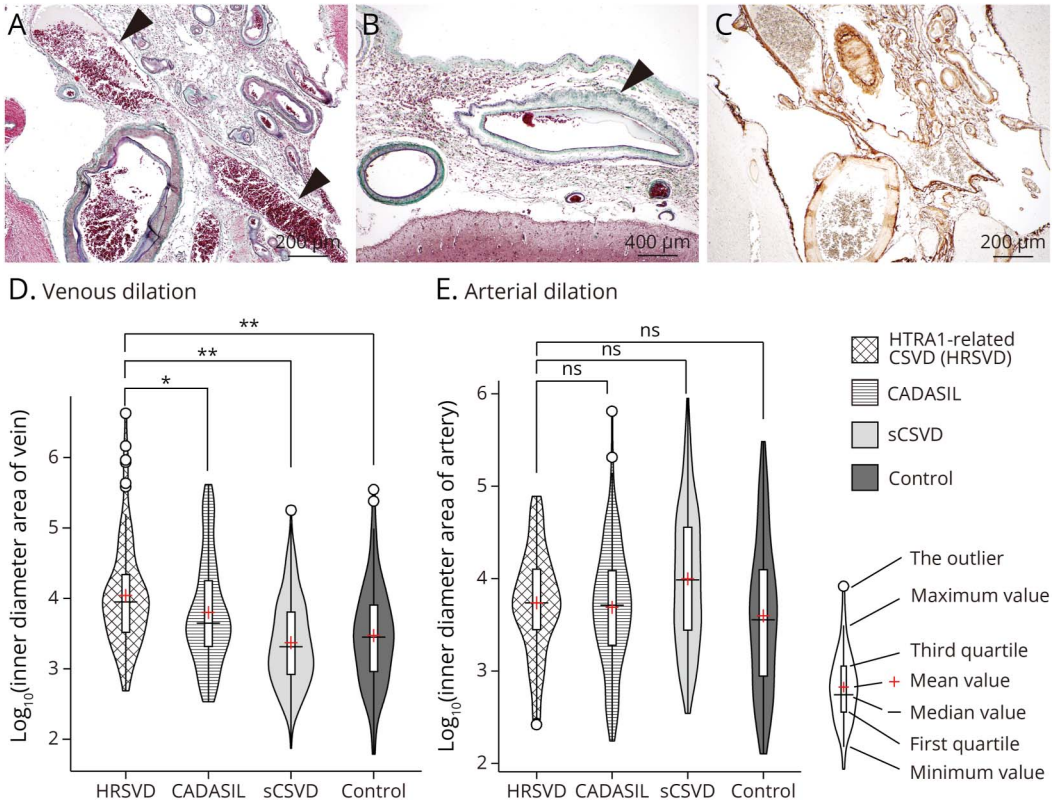

Photomicrographs of the leptomeningeal vessels of the midbrain in representative cases of HTRA1-related cerebral small vessel disease (HRSVD; A, C: case 1) and temporal tip in HRSVD (B: case 2). A list of patients is provided in eTable 3. (A, B) Disproportional enlargement of the leptomeningeal veins (arrowheads) relative to the adjacent arteries at the midbrain (A) and the temporal tip (B). (C) Type III collagen is deposited within the venous and arterial walls. (D, E) Distribution of venous (D) and arterial (E) lumen diameters in each group showed a significant venous dilation in patients with HRSVD. *$p = 0.05$, **$p < 0.001$. (A, B) Elastica-Goldner staining. (C) Immunohistochemical analysis of type III collagen. Scale bars = 200 μm in A and C and 400 μm in B. CADASIL = cerebral autosomal recessive arteriopathy with subcortical infarcts and leukoencephalopathy; ns = not significant; sCSVD = sporadic cerebral small vessel disease.

SWI protocols across institutions. It is crucial not only to align MRI parameters but also to perform minimum intensity projection to illustrate venous continuity.[37] Furthermore, setting a susceptibility threshold could help differentiate veins from cerebral microbleeds and reduce interobserver variability.[38] Third, longitudinal data of Chocolate Chip Sign are currently lacking. We were unable to find a correlation between the number of low-signal dots around the midbrain and disease duration in the HRSVD group. However, caution is required when interpreting these results because of the small sample size and the absence of direct intrapatient measurements. The longitudinal study incorporating clinical symptoms, other CSVD markers on MRI, and the Chocolate Chip Sign may help elucidate its potential utility as a prognostic biomarker.

In conclusion, the Chocolate Chip Sign represents a significant step toward understanding and diagnosing HRSVD. Its potential as both a diagnostic biomarker and a window into the underlying pathophysiology of the disease holds promise for improving the clinical management and treatment of this debilitating condition.

Acknowledgment

The authors appreciated the cooperation of the following physicians in this study: Akiyoshi Morinaga from Department of Neurology, Kanazawa University Graduate School of Medical Sciences; Chieko Suzuki from Department of Neurology, Hirosaki University Hospital; Eizo Tanaka from Department of Neurology, Kyushu University; Hiroaki Nozaki from Department of Neurology, Niigata City Hospital; Hiroko Kimura from Department of Neurology, Osaka General Hospital of West Japan Railway Company; Hiromasa Matsuno from Department of Neurology, The Jikei University School of Medicine; Hiromu Minagawa from Department of Neurology, Takagi Hospital; Kaneda Daita from Institute of Neuropathology, Fukushimura Hospital; Katsuki Eguchi from Department of Neurology, Hokuyukai Neurological Hospital; Kazuhide Miyazaki from Takada Clinic; Kei Tachibana from Department of Neurology, Suzuka Kaisei Hospital; Ko Matsuo from Department of Neurology, Japanese Red Cross Ise Hospital; Kosei Nakamura from Department of Neurology, Niigata University; Lee Jin-Hyung from Department of Neurology, Koshin University Gospel Hospital; Masahiro Mizobuchi from Department of Neurology, Nakamura Memorial Hospital; Mizuki Kanemoto

and Natsuko Iizuka from Department of Neurology, Showa University East Hospital; Naoki Yoshino from Department of Neurology, Hokushin General Hospital; Naoki Oyama from Department of Stroke Medicine, Kawasaki Medical School; Naoki Tosaka from Department of Neurology, University of Tsukuba; Shintaro Sugiyama from Department of Neurology, Sakai City Medical Center; Tetsuya Miyagi from Oroku Central Clinic; Tomone Taneda from Department of Neurology, Sadosogo Hospital; Toshiyasu Ogata from Department of Neurology, Japanese Red Cross Fukuoka Hospital; Veeramani Preethish-Kumar from Department of Neurology, Neurofoundation hospitals; Yasutaka Murakami from Department of Neurology, Osaka Police Hospitals; Yuji Isono from Department of Neurology, Nagoya City University East Medical Center; Yuma Shiomi from Department of Neurology, National Cerebral and Cardiovascular Center; Zenshi Miyake from Department of Neurology, NTT Medical Center Tokyo.

Author Contributions

S. Ando: drafting/revision of the manuscript for content, including medical writing for content; major role in the acquisition of data; study concept or design; analysis or interpretation of data. R. Saito: drafting/revision of the manuscript for content, including medical writing for content; major role in the acquisition of data; study concept or design; analysis or interpretation of data. S. Kitahara: major role in the acquisition of data. M. Uemura: study concept or design. Y. Hatano: analysis or interpretation of data. M. Watanabe: major role in the acquisition of data; analysis or interpretation of data. T. Kato: major role in the acquisition of data; analysis or interpretation of data. Y. Ito: major role in the acquisition of data; analysis or interpretation of data. A. Nalini: study concept or design. T. Ishihara: study concept or design. S. Murayama: study concept or design. H. Igarashi: study concept or design. A. Kakita: study concept or design. O. Onodera: drafting/revision of the manuscript for content, including medical writing for content; study concept or design.

Study Funding

This study was supported by the Japan Society for the Promotion of Science, Grants-in-Aid for Scientific Research (Grant Numbers JP 20K16595, JP 22H00466, JP 22H04923, JP 22K20882; Japan Agency for Medical Research and Development under Grant Number JP21wm0425019; and Japanese Ministry of Health, Labor, and Welfare, Grants-in-Aid for Research on Intractable Disease, Grant Number JP21FC1007).

Disclosure

Osamu Onodera is a speaker honorarium for the Kyowa Hakko Kirin Co. Ltd., Bristol-Myers Ltd., Ono Pharmaceutical Co. Ltd., Mitsubishi Ltd., Tanabe Pharm, Takeda, Daiichi-Sankyo, FUJIFILM, SANOFI, and FP-Pharm. The other authors have no conflicts of interest to declare. Go to Neurology.org/NG for full disclosures.

Publication History

Received by *Neurology: Genetics* August 5, 2024. Accepted in final form December 2, 2024. Submitted and externally peer reviewed. The handling editor was Associate Editor Alexandra Durr, MD, PhD.

References

1. Pantoni L. Cerebral small vessel disease: from pathogenesis and clinical characteristics to therapeutic challenges. *Lancet Neurol*. 2010;9(7):689-701. doi:10.1016/S1474-4422(10)70104-6
2. Hara K, Shiga A, Fukutake T, et al. Association of HTRA1 mutations and familial ischemic cerebral small-vessel disease. *N Engl J Med*. 2009;360(17):1729-1739. doi:10.1056/NEJMoa0801560
3. Malik R, Chauhan G, Traylor M, et al. Multiancestry genome-wide association study of 520,000 subjects identifies 32 loci associated with stroke and stroke subtypes. *Nat Genet*. 2018;50(4):524-537. doi:10.1038/s41588-018-0058-3
4. Nozaki H, Kato T, Nihonmatsu M, et al. Distinct molecular mechanisms of HTRA1 mutants in manifesting heterozygotes with CARASIL. *Neurology*. 2016;86(21):1964-1974. doi:10.1212/WNL.0000000000002694
5. Uemura M, Nozaki H, Kato T, et al. HTRA1-related cerebral small vessel disease: a review of the literature. *Front Neurol*. 2020;11:545. doi:10.3389/fneur.2020.00545
6. Uemura M, Nozaki H, Koyama A, et al. HTRA1 mutations identified in symptomatic carriers have the property of interfering the trimer-dependent activation cascade. *Front Neurol*. 2019;10:693. doi:10.3389/fneur.2019.00693
7. Verdura E, Herve D, Scharrer E, et al. Heterozygous HTRA1 mutations are associated with autosomal dominant cerebral small vessel disease. *Brain*. 2015;138(Pt 8):2347-2358. doi:10.1093/brain/awv155
8. Nozaki H, Sekine Y, Fukutake T, et al. Characteristic features and progression of abnormalities on MRI for CARASIL. *Neurology*. 2015;85(5):459-463. doi:10.1212/WNL.0000000000001803
9. Nozaki H, Nishizawa M, Onodera O. Features of cerebral autosomal recessive arteriopathy with subcortical infarcts and leukoencephalopathy. *Stroke*. 2014;45(11):3447-3453. doi:10.1161/STROKEAHA.114.004236
10. Rudilosso S, Chui E, Stringer MS, et al. Prevalence and significance of the vessel-cluster sign on susceptibility-weighted imaging in patients with severe small vessel disease. *Neurology*. 2022;99(5):e440-e452. doi:10.1212/WNL.0000000000200614
11. Chen X, Wei L, Wang J, et al. Decreased visible deep medullary veins is a novel imaging marker for cerebral small vessel disease. *Neurol Sci*. 2020;41(6):1497-1506. doi:10.1007/s10072-019-04203-9
12. Ishiyama H, Kim H, Saito S, et al. Pro-hemorrhagic cerebral autosomal dominant arteriopathy with subcortical infarcts and leukoencephalopathy associated with NOTCH3 p.R75P mutation with low vascular NOTCH3 aggregation property. *Ann Neurol*. 2024;95(6):1040-1054. doi:10.1002/ana.26916
13. Uemura M, Hatano Y, Nozaki H, et al. High frequency of HTRA1 AND ABCC6 mutations in Japanese patients with adult-onset cerebral small vessel disease. *J Neurol Neurosurg Psychiatry*. 2023;94(1):74-81. doi:10.1136/jnnp-2022-329917
14. Fazekas F, Chawluk JB, Alavi A, Hurtig HI, Zimmerman RA. MR signal abnormalities at 1.5 T in Alzheimer's dementia and normal aging. *AJR Am J Roentgenol*. 1987;149(2):351-356. doi:10.2214/ajr.149.2.351
15. Frangi AF, Niessen WJ, Vincken KL, Viergever MA. Multiscale vessel enhancement filtering. In: Wells WM, Colchester A, Delp S, eds. *Medical Image Computing and Computer-Assisted Intervention—MICCAI'98*. Springer Berlin Heidelberg; 1998:130-137.
16. Zivadinov R, Poloni GU, Marr K, et al. Decreased brain venous vasculature visibility on susceptibility-weighted imaging venography in patients with multiple sclerosis is related to chronic cerebrospinal venous insufficiency. *BMC Neurol*. 2011;11:128. doi:10.1186/1471-2377-11-128
17. Isensee F, Schell M, Pflueger I, et al. Automated brain extraction of multisequence MRI using artificial neural networks. *Hum Brain Mapp*. 2019;40(17):4952-4964. doi:10.1002/hbm.24750
18. Nakada T, Matsuzawa H, Igarashi H, Fujii Y, Kwee IL. In vivo visualization of senile-plaque-like pathology in Alzheimer's disease patients by MR microscopy on a 7T system. *J Neuroimaging*. 2008;18(2):125-129. doi:10.1111/j.1552-6569.2007.00179.x
19. Nakada T, Matsuzawa H, Igarashi H, Kwee IL. Expansion of corticomedullary junction high-susceptibility region (CMJ-HSR) with aging: a clue in the pathogenesis of Alzheimer's disease?. *J Neuroimaging*. 2012;22(4):379-383. doi:10.1111/j.1552-6569.2011.00607.x
20. Haacke EM, Xu Y, Cheng YC, Reichenbach JR. Susceptibility weighted imaging (SWI). *Magn Reson Med*. 2004;52(3):612-618. doi:10.1002/mrm.20198
21. Reichenbach JR, Barth M, Haacke EM, Klarhofer M, Kaiser WA, Moser E. High-resolution MR venography at 3.0 tesla. *J Comput Assist Tomogr*. 2000;24(6):949-957. doi:10.1097/00004728-200011000-00023
22. Montine TJ, Phelps CH, Beach TG, et al. National Institute on Aging-Alzheimer's Association guidelines for the neuropathologic assessment of Alzheimer's disease: a practical approach. *Acta Neuropathol*. 2012;123:1-11. doi:10.1007/s00401-011-0910-3
23. McKeith IG, Boeve BF, Dickson DW, et al. Diagnosis and management of dementia with Lewy bodies: fourth consensus report of the DLB Consortium. *Neurology*. 2017;89(1):88-100. doi:10.1212/WNL.0000000000004058
24. Olichney JM, Hansen LA, Hofstetter CR, Grundman M, Katzman R, Thal LJ. Cerebral infarction in Alzheimer's disease is associated with severe amyloid

angiopathy and hypertension. *Arch Neurol*. 1995;52(7):702-708. doi:10.1001/archneur.1995.00540310076019
25. Yamamoto Y, Ihara M, Tham C, et al. Neuropathological correlates of temporal pole white matter hyperintensities in CADASIL. *Stroke*. 2009;40(6):2004-2011. doi:10.1161/STROKEAHA.108.528299
26. Kato T, Manabe RI, Igarashi H, et al. Candesartan prevents arteriopathy progression in cerebral autosomal recessive arteriopathy with subcortical infarcts and leukoencephalopathy model. *J Clin Invest*. 2021;131(22):e140555. doi:10.1172/JCI140555
27. Moody DM, Brown WR, Challa VR, Anderson RL. Periventricular venous collagenosis: association with leukoaraiosis. *Radiology*. 1995;194(2):469-476. doi:10.1148/radiology.194.2.7824728
28. Brown WR, Moody DM, Challa VR, Thore CR, Anstrom JA. Venous collagenosis and arteriolar tortuosity in leukoaraiosis. *J Neurol Sci*. 2002;203-204:159-163. doi:10.1016/s0022-510x(02)00283-6
29. Murwantoko YanoM, Yano M, Ueta Y, et al. Binding of proteins to the PDZ domain regulates proteolytic activity of HtrA1 serine protease. *Biochem J*. 2004;381(Pt 3):895-904. doi:10.1042/BJ20040435
30. Cai M, Zhang XF, Qiao HH, et al. Susceptibility-weighted imaging of the venous networks around the brain stem. *Neuroradiology*. 2015;57(2):163-169. doi:10.1007/s00234-014-1450-z
31. Charidimou A, Boulouis G, Frosch MP, et al. The Boston criteria version 2.0 for cerebral amyloid angiopathy: a multicentre, retrospective, MRI-neuropathology diagnostic accuracy study. *Lancet Neurol*. 2022;21(8):714-725. doi:10.1016/S1474-4422(22)00208-3
32. Hatano T, Daida K, Hoshino Y, et al. Dystonia due to bilateral caudate hemorrhage associated with a COL4A1 mutation. *Parkinsonism Relat Disord*. 2017;40:80-82. doi:10.1016/j.parkreldis.2017.04.009
33. Malik R, Beaufort N, Frerich S, et al. Whole-exome sequencing reveals a role of HTRA1 and EGFL8 in brain white matter hyperintensities. *Brain*. 2021;144(9):2670-2682. doi:10.1093/brain/awab253
34. Houck AL, Gutierrez J, Gao F, et al. Increased diameters of the internal cerebral veins and the basal veins of rosenthal are associated with white matter hyperintensity volume. *AJNR Am J Neuroradiol*. 2019;40(10):1712-1718. doi:10.3174/ajnr.A6213
35. Zhang W, Zhou Y, Wang J, et al. Glymphatic clearance function in patients with cerebral small vessel disease. *Neuroimage*. 2021;238:118257. doi:10.1016/j.neuroimage.2021.118257
36. Haacke EM, Liu S, Buch S, Zheng W, Wu D, Ye Y. Quantitative susceptibility mapping: current status and future directions. *Magn Reson Imaging*. 2015;33:1-25. doi:10.1016/j.mri.2014.09.004
37. Halefoglu AM, Yousem DM. Susceptibility weighted imaging: clinical applications and future directions. *World J Radiol*. 2018;10(4):30-45. doi:10.4329/wjr.v10.i4.30
38. Liu S, Buch S, Chen Y, et al. Susceptibility-weighted imaging: current status and future directions. *NMR Biomed*. 2017;30(4). doi:10.1002/nbm.3552